

Article

## Integrated Biophotonics with CYTOP

Kristjan Leosson <sup>1,\*</sup> and Björn Agnarsson <sup>2</sup>

<sup>1</sup> Department of Physics, Science Institute, University of Iceland, Dunhagi 3, IS107 Reykjavik, Iceland

<sup>2</sup> Department of Applied Physics, Chalmers University of Technology, SE-41296 Gothenburg, Sweden

\* Author to whom correspondence should be addressed; E-Mail: kleos@hi.is; Tel.: +354-525-4800; Fax: +354-552-8911.

Received: 24 January 2012; in revised form: 16 February 2012 / Accepted: 20 February 2012 /

Published: 29 February 2012

---

**Abstract:** We describe how the amorphous fluoropolymer CYTOP can be advantageously used as a waveguide cladding material in integrated optical circuits suitable for applications in integrated biophotonics. The unique refractive index of CYTOP ( $n = 1.34$ ) enables the cladding material to be well index-matched to an optically probed sample solution. Furthermore, ultra-high index contrast waveguides can be fabricated, using conventional optical polymers as waveguide core materials, offering a route to large-scale integration of optical functions on a single chip. We discuss applications of this platform to evanescent-wave excitation fluorescence microscopy, passive and/or thermo-electrically-controlled on-chip light manipulation, on-chip light generation, and direct integration with microfluidic circuits through low-temperature bonding.

**Keywords:** lab-on-a-chip; fluorescence microscopy; integrated biophotonics; polymer waveguides; fluoropolymers; biosensors; microfluidics

---

### 1. Introduction

Deployment of integrated waveguide optics (or planar lightwave circuits, PLCs) has gone hand-in-hand with the explosive growth in fiber-optic communications, starting in the early 1990s, and integrated optical components are now ubiquitous in optical networks [1]. Due to the strict reliability criteria imposed by the telecommunications industry, PLCs have traditionally been fabricated using inorganic materials (glasses/oxides/semiconductors). Through great development efforts, however, polymer-based waveguide components satisfying Telcordia standards have also been realized and

marketed, mainly in order to exploit the large thermo-optic coefficient of polymers for reducing electrical power consumption in large-scale thermo-optic attenuator/switching arrays [2–4]. In recent years, PLCs are increasingly being employed for sensing and monitoring applications, where waveguide circuits are often combined with electrical, microfluidic and/or micromechanical components in complex lab-on-a-chip devices for (bio)chemical analysis [5]. In this case, polymers are highly suitable as a waveguide platform, offering a wide range of optical, physical and chemical properties, biocompatibility, low cost and a large variety of possible processing and patterning techniques, with less emphasis on long-term reliability and global component standardization. Application of integrated optical techniques in biological analysis (integrated biophotonics), includes functions such as on-chip fluorescence excitation and/or detection, optical manipulation (e.g., optical tweezers) and label-free sensing (based on, e.g., Raman scattering or refractive-index monitoring) [6].

One of the interesting properties of optical polymers is the wide range of refractive index values of commercially available materials [7], from below  $n = 1.3$  to above  $n = 1.7$ . Transparent polymers with  $n = 1.33$ – $1.36$  are particularly interesting for biophotonics applications, as their refractive index lies in the same range as that of typical samples under study, which may consist mainly of water, buffer solution and/or liquids of biological origin (such as blood plasma or intracellular fluid). Only very few optical polymers in this index range are available. In contrast, common transparent polymers such as poly(methyl methacrylate), polystyrene or polycarbonate have refractive index values in the range 1.49–1.59.

The amorphous perfluorinated polymer CYTOP (Asahi Glass Co. Ltd.) is particularly suitable for applications in integrated biophotonics. CYTOP has a refractive index of 1.34 (at  $\lambda = 589$  nm), low chromatic dispersion (Abbe number = 90) and high transparency from 200 nm to beyond 2,000 nm wavelength. Generally, fluoropolymers exhibit strong chemical resistance, non-toxicity and resistance to biodegradation [8]. CYTOP is soluble in fluorinated solvents and can be cast into thin (few  $\mu\text{m}$  or less) films by, e.g., spin coating or dip coating, or molded by, e.g., extrusion or injection molding. It is used for a variety of applications due to its special optical, electrical, physical and chemical characteristics, including anti-reflection coatings, moisture barriers, super-hydrophobic surfaces, photomask pellicles, graded-index polymer optical fibers, in microfluidics and wafer bonding, and as an interlayer dielectric [9–17].

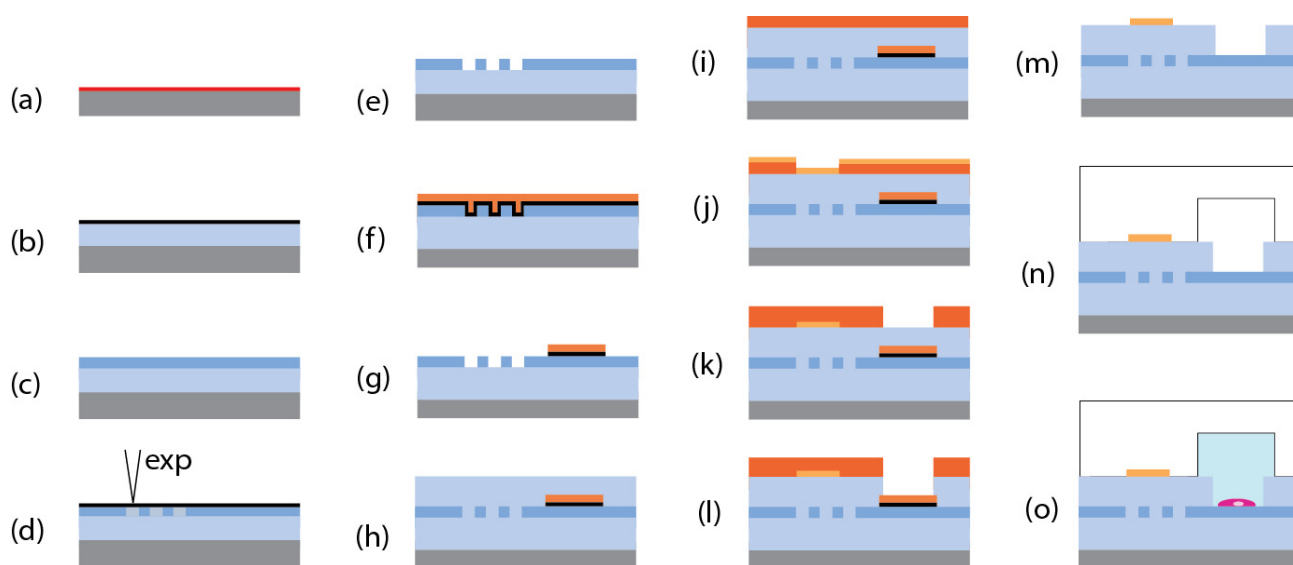
In spite of its excellent optical characteristics, the use of CYTOP in PLC fabrication for biophotonics is still not widespread, presumably due to fabrication issues. Even though significant bond strength has been reported for high-pressure wafer bonding with CYTOP at temperatures exceeding the glass transition temperature [15], the untreated surface of CYTOP is hydrophobic and securing adhesion in multi-layer photonic structures, such as slab waveguides, can be difficult. Such structures may deform if the process temperature exceeds  $T_g$ , which for CYTOP is 108 °C. As described in the present paper, however, these difficulties can be overcome, making CYTOP an interesting choice as a cladding material for a PLC platform for biophotonics, as the sample(s) under investigation can replace the cladding material in selected sensing areas without introducing a significant degree of optical discontinuity. Furthermore, slab, ridge or channel waveguide cores can be fabricated using conventional spin-on polymers with a refractive index around  $n = 1.5$ . This results in an ultra-high (10–15%) index contrast waveguide platform (according to the classification given in [18]), having a practically lossless single-mode waveguide bend radius below 100  $\mu\text{m}$  and overall

component sizes that can be orders of magnitude smaller than in standard glass-based integrated optics [18], with the ability to confine light on a length scale that matches the maximum resolution of conventional far-field imaging system, such as an optical microscope.

## 2. Fabrication

The process steps that we have developed for fabricating waveguide chips containing CYTOP are outlined in this section. All processing was carried out in a class-100 cleanroom, using precision-filtered polymer solutions, as contamination of the guiding layers can have very detrimental effects on device performance. Figure 1 illustrates a possible fabrication process for a biophotonic chip involving thermo-electric control and microfluidic circuits for introducing a sample solution.

**Figure 1.** Process flow for fabricating a biophotonic chip with CYTOP waveguide cladding (structures are not to scale). **(a)** Substrate pretreatment; **(b)** CYTOP coating and Al deposition; **(c)** Al removal and coating with waveguide core polymer; **(d)** Patterning of waveguide core polymer by UV or e-beam exposure; **(e)** Development of exposed pattern; **(f)** Deposition of protective layer (if needed) and etch stop photoresist; **(g)** Patterning and development of etch stop layer; **(h)** Coating with top CYTOP cladding; **(i)** Contact layer resist coating; **(j)** Patterning, development, metallization and liftoff; **(k)** Application, patterning and development of etch mask layer; **(l)** Reactive ion etching of sample wells; **(m)** Photoresist and Al protective layer removal; **(n)** APTES treatment and bonding of standard PDMS microfluidic circuits to the CYTOP coated chip; **(o)** Introduction of the (biological) sample.



A substrate (e.g., silicon or glass) is heated to remove moisture and spin-coated with a silane coupling agent in solution. For all our waveguide chips, we used A-grade CYTOP with  $-\text{COOH}$  end-groups. A different type of CYTOP (M-grade,  $-\text{CONH}\sim\text{SiOR}$  end-groups) provides direct adhesion to inorganic substrate without silane pretreatment. However, in our experience, the M-grade did not exhibit sufficient mechanical stability to yield good end facets upon dicing (to enable efficient end-fire coupling of light to the waveguides from optical fibers). A filtered CYTOP solution (CTX-809AP2)

was spin-coated on the surface, yielding a thickness of 4  $\mu\text{m}$  at 1,000 rpm spin speed. In order to ensure a flat CYTOP surface for this thickness range, it is crucial to carefully control the polymer baking process. Our wafers were typically placed in a programmable cleanroom oven under a glass cover to slow down solvent evaporation and kept at 50 °C for 30 min, followed by gentle ramping to a baking temperature of 180 °C and baking for 1 h, before allowing to cool down inside the oven. The resulting CYTOP surface is flat (<10 nm surface roughness measured by a profilometer) and hydrophobic (measured contact angle around 110°). We have studied the effect of plasma treatment on the wettability of the CYTOP surface, for different plasma conditions [19]. Several minutes in Ar plasma can reduce the contact angle to below 60°. However, we found that such treatment did not ensure sufficient adhesion to subsequent layers. An efficient method to ensure both wettability and good adhesion is the deposition of a thin Al layer on the CYTOP surface, resulting in interactions between aluminol sites and the carbonyl functional groups [20] as well as possible ionic bonding between the carboxylate anion of the CYTOP end-group and the aluminum. Upon removal of the Al layer by wet etching in an alkaline solution, the end-groups of the polymer remain oriented towards the polymer surface and the contact angle is reduced to 80°. For waveguide core layers, we have successfully experimented with a variety of common optical polymer materials, including PMMA, polystyrene, BCB, ORMOCERs, SU8 and various conjugated fluorescent polymer blends. The waveguide core layer can, in some cases, be directly patterned using UV photolithography and/or electron-beam lithography, depending on the particular material used. In other cases, waveguides can be patterned using an additional patternable soft etch mask layer and dry etching. In most of our work, we have used 950PMMA-A (MicroChem), which is directly patternable by e-beam exposure, as a waveguide core layer. The PMMA was coated with a thin layer of Al prior to e-beam exposure to prevent charging and the Al layer was wet-etched in alkaline solution before developing the exposed PMMA.

For excitation/sensing purposes, the sample solution should preferably be in direct contact with the waveguide core. Omitting a top cladding layer and covering the entire chip with the sample solution is neither experimentally practical nor conducive to large-scale integration. Therefore, the top cladding must be completely etched away in pre-defined areas, without disturbing the waveguide core layer. An etch stop layer of photoresist was therefore patterned on top of the waveguide layer, following deposition of a thick (200 nm) Al layer in cases where the waveguide core material had to be protected from the photoresist solvent to avoid deterioration of optical properties (as in the case of PMMA). A second 4  $\mu\text{m}$  CYTOP coating was applied on top of the waveguide layer with etch stops. A substantially reduced baking temperature of 100 °C was used for the top cladding, in order to prevent deformation of the waveguide structure.

As mentioned in the previous section, polymer materials are well-suited for fabricating thermo-optic components, due to the fact that their variation in refractive index with temperature is typically an order of magnitude larger than in common inorganic dielectrics. In polymers, the thermo-optic coefficient ( $dn/dT$ ) is negative and mainly attributable to thermal volume expansion. We have fabricated electrically controlled optical attenuators using the CYTOP-PMMA-CYTOP platform, using heating elements on the top cladding layer [21]. Heating elements can be patterned on the top cladding surface as illustrated in Figure 1, using Al deposition and removal, photoresist patterning, metal deposition (typically gold) and liftoff in an alkaline photoresist remover.

Sample wells are formed by reactive ion etching (RIE) of the CYTOP top cladding. A soft etch mask (photoresist) was used to pattern the sample wells. Etching was carried out using an O<sub>2</sub>:CHF<sub>3</sub> (20:60 sccm) plasma at 100 W RF power and 15 mtorr, giving an etch rate of about 140 nm/min for CYTOP which is around two times larger than the etch rate of the photoresist used (maN-1420, micro resist technology GmbH). Directly after etching down to the etch stop layer, wafers were typically diced (to take advantage of the surface protection provided by the remaining photoresist) and finally rinsed in an alkaline photoresist remover which also served to etch away the protective Al layer on top of the waveguide core.

Depending on the particular application, the sample well can be left open (e.g., for giving access to a culture medium in live-cell evanescent-wave imaging experiments, using an inverted microscope and a thin transparent substrate), filled with a sample solution and closed with a silicone seal and microscope cover slip (as in [22]), or alternatively (as shown in Figure 1) attached to a conventional PDMS microfluidic circuit. For irreversibly bonding PDMS to the CYTOP surface, we adopted the approach reported by Vlachopoulou *et al.* for attaching PDMS to organic polymers [23]. A PDMS (Dow Corning SYLGARD 184) microfluidic circuit with 40- $\mu$ m high and 100- $\mu$ m wide channels was cast using a separately patterned SU-8 mold. The CYTOP surface was prepared using O<sub>2</sub>/Ar plasma treatment, followed by aminopropyltriethoxysilane (APTES) coating and baking at 80 °C for 30 min. The APTES-coated CYTOP surface and the PDMS were treated in O<sub>2</sub>/Ar plasma for 1 min in a Plasma-Preen system, attached (following a short exposure to air) and left for 1 h. A strong bond was obtained and no leakage or delamination was observed when liquid was pumped through the circuit, from an externally pressurized reservoir.

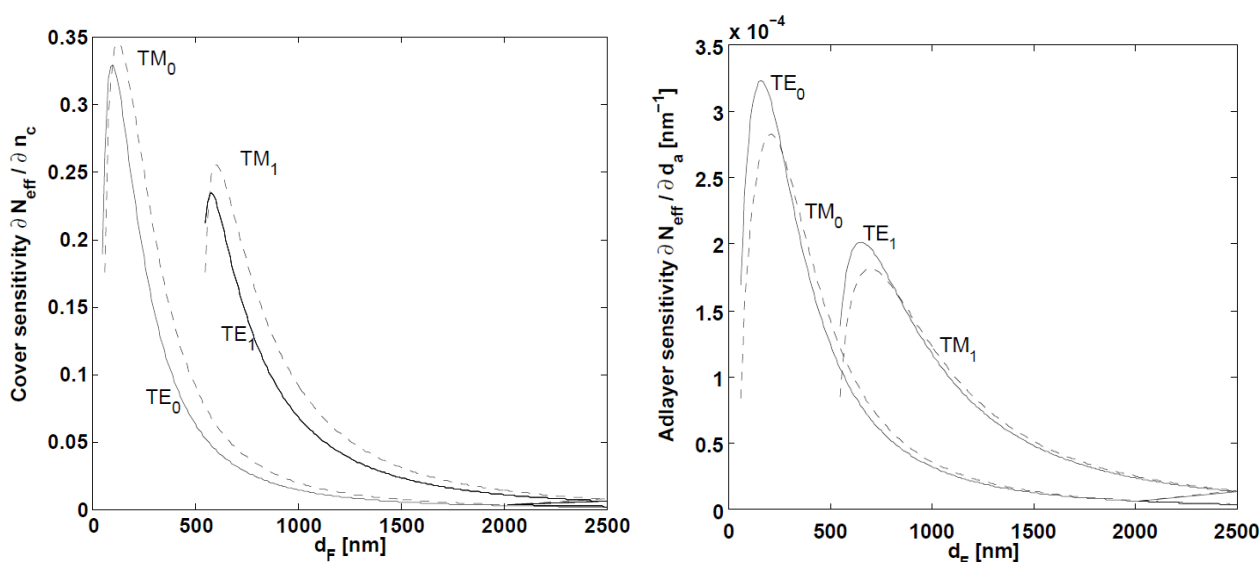
### 3. Results and Discussion

Buried channel waveguides supporting only the fundamental TM<sub>00</sub> and TE<sub>00</sub> modes (simply referred to as “single-mode” waveguides below) can be fabricated using the waveguide platform described in the previous section, provided that the waveguide core layer can be patterned to sub-micron dimensions. As an example, square-cross-section PMMA channels in CYTOP with core sizes in the range 300 nm to 500 nm exhibit single-mode behavior across the visible wavelength range [24]. Such transverse dimensions are easily obtained by spin-coating and lateral dimension are within the capabilities of e-beam or DUV lithography, both of which can be used to pattern the PMMA layer.

In some cases, a slab waveguide consisting of a uniform layer of high-index polymer is sufficient for specific functions, such as providing wide-field illumination for evanescent-wave microscopy [22], monitoring of surface-bound fluorescent markers or functionalized metal nanoparticles, or for refractive index sensing. Here, CYTOP plays a crucial role in extending the range of possible penetration depths of the excitation field, controlled by varying the waveguide core layer thickness and/or refractive index. For the same reason, so-called reverse symmetry waveguides fabricated on special low-index porous glass substrates ( $n = 1.2$ ) have been developed and used for refractive index sensing, as well as bacterial and cell monitoring applications [25–27]. For a completely symmetric three-layer waveguide there is no cutoff thickness for the core layer and any penetration depth of the evanescent field into the sample solution can, in principle, be realized. In a practical case, however, the sample (forming the top cladding) will not match the CYTOP (bottom cladding) refractive index

exactly, thus limiting the range of possible penetration depths. Nevertheless, the refractive index of CYTOP being close to that of typical biological samples extends this range well beyond what is possible with more conventional slab-waveguide systems, such as a high-index oxide on glass [28,29] and results in a larger fraction of the excitation power being carried in the evanescent tail on the sample side. For refractive index sensing, larger penetration depth gives improved sensitivity of the guided mode to the cover index [25]. Numerical results of refractive index and adlayer thickness sensitivity are plotted for the CYTOP-PMMA waveguide in Figure 2. Due to the increased penetration depth, refractive index sensitivity is increased, whereas adlayer thickness sensitivity is slightly decreased, compared to e.g., the high-index oxide waveguide on glass discussed in [30].

**Figure 2.** Calculated sensitivities for a refractive index sensor based on the PMMA-CYTOP slab waveguide platform (633 nm operating wavelength). Sensitivity of the guided mode index to the refractive index of the cover layer (**left**) and the thickness of an adsorbed layer with an index of  $n = 1.5$  (**right**), plotted for different thickness of the waveguide core layer,  $d_F$ .

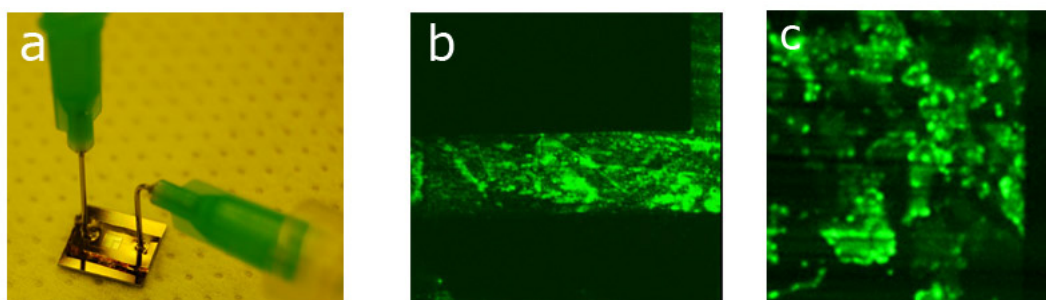


In the case where the evanescent part of the guided wave is used to excite fluorescent labels for surface-specific microscopy, we have referred to our approach as Symmetric-Waveguide-Excitation Fluorescence Microscopy (SWExFM) [22]. Waveguide excitation represents a chip-based alternative to total internal reflection fluorescence (TIRF) microscopy, where evanescent-wave excitation at the glass-sample interface is provided using high-NA objective lenses on inverted microscopes. TIRF was introduced in the early 1990s and has since been steadily gaining in popularity. While TIRF generally provides stronger confinement of the excitation light, the SWExFM technique has a number of important advantages, as it decouples the excitation and imaging optics and provides more flexibility with respect to substrate types, range of penetration depths and size of the illuminated field. Examples of fluorescently labeled cells cultured on CYTOP-PMMA waveguide chips can be found in [19,21,22]. These measurements reveal details of the near-surface region, undisturbed by out-of-focus background fluorescence arising from the bulk of the cell cluster (as would be the case in conventional epi-fluorescence microscopy). The evanescent-wave excitation, combined with an optimized excitation

wavelength (supercontinuum source filtered by acousto-optic tunable filter) and a highly sensitive camera, ensures a very low degree of photobleaching of the samples during imaging, as compared to a conventional epi-fluorescence microscope system.

Figure 3(a) shows a separately patterned PDMS microfluidic circuit with 40- $\mu\text{m}$  deep channels bonded to the waveguide chip. As described in the previous section, we used APTES-coating and oxygen plasma treatment to secure a strong CYTOP-PDMS bond. In Figure 3(b), fluorescence from polymer beads (Invitrogen FluoSpheres) in water suspension passing through the microfluidic channel is depicted. Similarly, the near-surface region of live cells expressing a green fluorescent protein (GFP) can be imaged using the evanescent-wave excitation, as shown for transfected pig kidney epithelial (LLC PK1) cells in Figure 3(c). For applications such as time-lapse imaging of live cells, the excitation can be modulated using on-chip thermo-optic control with a high extinction ratio and sub-ms response time, as discussed in more detail in [21].

**Figure 3.** (a) CYTOP-PMMA-CYTOP waveguide chip bonded to a PDMS microfluidic circuit. A square-shaped sensing area is visible in the center of the chip; (b) False-color image of fluorescent beads in water solution passing through a 100  $\mu\text{m}$  wide microfluidic channel above the sensing area. The penetration depth of the evanescent field into the solution is around 200 nm; (c) Live dSH2-GFP-expressing cells at the edge of the sensing area. The GFP attaches to focal adhesions in the cells.

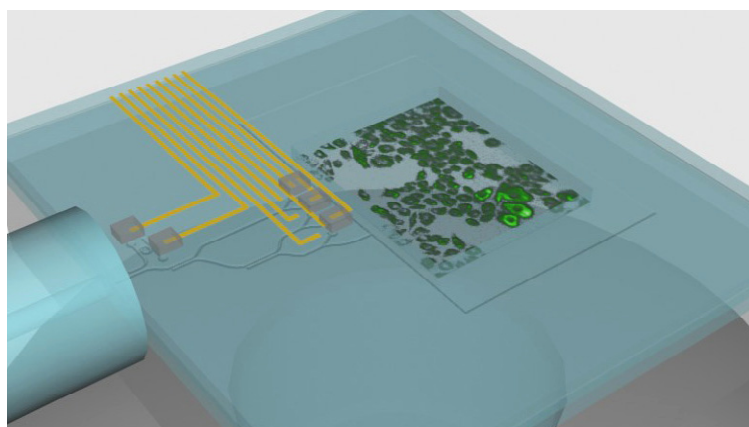


By patterning the waveguide core layer to form single-mode channel waveguides, a wide range of optical components can be realized, including passive devices such as power splitters, interferometers, resonators, grating filters (e.g., waveguide Bragg reflectors or arrayed waveguide gratings), polarization filters, and in/out-couplers. On one hand, passive devices can serve to distribute and filter excitation light on a biochip, where fluorescence or scattering from, e.g., surface-bound analytes or tagged proteins in a cell culture is measured with separate optics. The monitoring of light transmission through passive devices, on the other hand, can be used for refractive-index or temperature sensing, or monitoring of near-surface fluorescence directly coupled into the waveguide mode. In our previous work, we have reported the performance of several passive PMMA-CYTOP waveguide devices, including splitters, couplers and resonators [24].

More sophisticated manipulation is obtained by electrically controlling the propagation of light on the chip. For modulation time scales of the order of 1 ms, this is most easily done by modulating the effective refractive index of the waveguide mode by changing the local temperature of the waveguide. Faster signal modulation is also possible, through careful device optimization or the use of other modulation principles (e.g., electro-optic polymers). Recently, we demonstrated efficient on-off

switching for time-lapse fluorescence imaging using a thermo-electrically controlled interferometric device [21], consisting of a single Mach-Zehnder interferometer device with one arm heated to achieve constructive or destructive interference of the output mode. A 25-dB extinction ratio was realized at a driving power of only 10 mW. More complex devices based on similar operating principles can be readily envisioned (Figure 4). With a suitable wide-band single-mode (supercontinuum) light source, multi-wavelength probing/excitation with individually modulated channels can be realized by combining thermo-optic functions with passive filtering. Application examples include time-lapse live-cell imaging, high-speed multi-wavelength fluorescence imaging, and modulation-frequency-encoded multi-wavelength analysis [31]. Furthermore, thermo-optic devices can be used to for inducing variable phase shifts in, e.g., structured illumination microscopy.

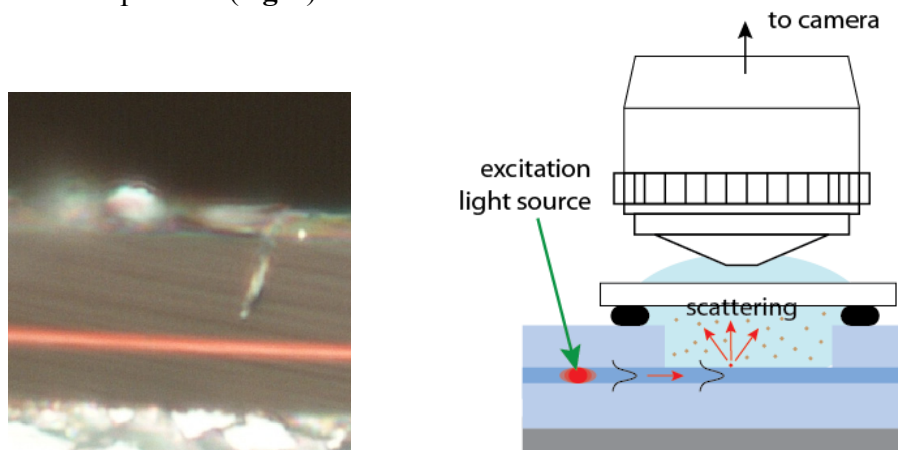
**Figure 4.** Simplified schematic view of a possible chip layout containing a single sample well, monitoring of fiber alignment and temperature, as well as splitting and individual shuttering of three excitation wavelengths using directional couplers and digital optical switches (micro-incubator assembly not shown). In the depicted set-up, fluorescence from cells in the sample well is collected from below using an inverted microscope objective.



In the previously mentioned work, light was introduced into the single-mode waveguides by manually aligning a tapered lensed optical fiber with a sub-micron focus spot size to the input waveguide [24]. This introduces stringent alignment tolerances, which are not practical for routine measurements or device packaging. Alternatively, a conventional single-mode fiber can be used, at the expense of larger coupling loss. These restrictions could be partly alleviated with adiabatic on-chip mode conversion, but ideally, light sources should be integrated directly on the chip. Such sources can consist of optically pumped fluorescent materials or electrically driven sources such as organic light-emitting diodes (OLEDs) [32].

In order to demonstrate the possibility of using a fluorescent waveguide layer for evanescent wave sensing, we replaced the PMMA core layer with a 200-nm thick layer of conjugated fluorescent polymer. In addition to providing a symmetric cladding environment, the CYTOP layer serves to protect the fluorescent polymer layer from degradation due to moisture [10]. The fluorescent polymer layer was excited in an area away from the sample well using a 5-mW CW laser as shown schematically in Figure 5.

**Figure 5.** A fluorescent waveguide layer sandwiched between two CYTOP layers acting as an on-chip optically-pumped light source. Red emission from the diced facet of the sample is clearly seen (**left**). The guided fluorescence was used to monitor motion on gold nanoparticles in suspension (**right**).



A dilute suspension of 100-nm gold nanoparticles in de-ionized water was introduced into the sample well. The scattering from particles within the evanescent field was collected using a microscope objective and imaged with a CCD camera. At the emission wavelength, the fluorescent polymer is transparent and acts as a high-index contrast waveguide core ( $n = 1.67$ ). Blinking of gold particles moving in and out of the light field provided clear evidence of evanescent wave excitation at the fluorescence wavelength. By introducing feedback into the polymer waveguide structure, optically pumped laser sources can be realized [33], improving substantially the efficiency of sample excitation.

#### 4. Conclusions

We have demonstrated that the amorphous fluoropolymer CYTOP can be used in a variety of integrated biophotonic devices. The refractive index of CYTOP, along with its compatibility with other polymers and with biological samples, gives many interesting possibilities for realizing compact biophotonic circuits. We presented procedures for fabricating components suitable for large-scale integration of optical functions, including electrically-controlled modulators and switches, as well as optically pumped on-chip light sources. Direct integration with PMDS microfluidic circuits was also successfully demonstrated. For aqueous samples, the symmetric cladding environment provides improved refractive-index sensitivity and greater control over the penetration of the evanescent field into the sample solution, as compared to conventional waveguide configurations using glass substrates. It offers an important addition to current evanescent-field microscopy methods for surface-specific investigations of biological samples, such as or monitoring of surface binding events.

#### Acknowledgments

The authors wish to thank those who have contributed to and inspired this work, including Jennifer Halldorsson, Nina B. Arnfinnsdottir, Asta B. Jonsdottir, Thorarinn Gudjonsson, Saevar Ingthorsson, Malte C. Gather, Gudmundur K. Stefansson, Dadi Bjarnason, Fredrik Höök, Anders Kristensen, Mads H. Sørensen, Thomas Nikolajsen and Sergey I. Bozhevolnyi.

The project has been supported by the Icelandic Science and Technology Policy Council (ISTPC) Framework Programme for Nanotechnology, the ISTPC Graduate Student Fund, the University of Iceland Research Fund, the Reykjavik Energy Environmental and Energy Research Fund and the Icelandic Student Innovation Fund.

## References

1. Keiser, G. *Optical Communication Essentials*; McGraw-Hill: New York, NY, USA, 2003.
2. Eldada, L. Polymer integrated optics: promise *versus* practicality. In *Organic Photonic Materials and Devices VII*, Grote J.G., Kaino, T., Kajzar, F., Eds.; SPIE: Bellingham, WA, USA, 2005; Volume 5724, pp. 96–106.
3. Cockroft, N. Array-based VOAs offer compact signal control. *WDM Solut.* **2001**, *3*, 81–86.
4. Noh, Y.-O.; Lee, C.-H.; Kim, J.-M.; Hwang, W.-Y.; Won, Y.-H.; Lee, H.-J.; Han, S.-G.; Oh, M.-C. Polymer waveguide variable optical attenuator and its reliability. *Opt. Commun.* **2004**, *242*, 533–540.
5. Li, P.C.H. *Microfluidic Lab-on-a-Chip for Chemical and Biological Analysis and Discovery*; CRC Press: Boca Raton, FL, USA, 2006.
6. Prasad, P.N. *Introduction to Biophotonics*; Wiley-Interscience: Hoboken, NJ, USA, 2003.
7. Eldada, L.; Schacklette, L.W. Advances in polymer integrated optics. *IEEE J. Sel. Top. Quantum Electron.* **2000**, *6*, 54–68.
8. Leis, A.P.; Schlicher, S.; Franke, H.; Strathmann, M. Optically transparent porous medium for nondestructive studies of microbial biofilm architecture and transport dynamics. *Appl. Environ. Microbiol.* **2005**, *71*, 4801–4808.
9. Yamamoto, K.; Ogawa, G. Structure determination of the amorphous perfluorinated homopolymer: Poly[perfluoro(4-vinyl-1-butene)]. *J. Fluor. Chem.* **2005**, *126*, 1403–1408.
10. Granstrom, J.; Swensen, J.S.; Moon, J.S.; Rowell, G.; Yuen, J.; Heeger, A.J. Encapsulation of organic light-emitting devices using a perfluorinated polymer. *Appl. Phys. Lett.* **2008**, *93*, 193304:1-193304:3.
11. Kobayashi, T.; Shimizu, K.; Kaizuma, Y.; Konishi, S. Formation of superhydrophobic/superhydrophilic patterns by combination of nanostructure-imprinted perfluoropolymer and nanostructured silicon oxide for biological droplet generation *Appl. Phys. Lett.* **2011**, *98*, 123706:1-123706:3.
12. Eynon, B.G.; Wu, B. *Photomask Fabrication Technology*; McGraw-Hill: New York, NY, USA, 2005.
13. Polishuk, P. Plastic optical fibers branch out. *IEEE Commun. Mag.* **2006**, *44*, 140–148.
14. Uchida, D.; Kanai, M.; Nishimoto, T.; Shoji, S. Fabrication of the perfluoro polymer passivated PDMS microstructure. *IEEE J. Trans. Sens. Micromach.* **2005**, *124*, 364–368.
15. Oh, K.W.; Han, A.; Bhansali, S.; Ahn, C.H. A low-temperature bonding technique using spin-on fluorocarbon polymers to assemble microsystems. *J. Micromech. Microeng.* **2002**, *12*, 187–191.
16. Jikuhara, R.; Tanahashi, S. A high performance MCM-D using Cu/fluoropolymer thin film multilayer technology. In *Proceedings of 1995 Electrical Performance of Electronic Packaging*, Portland, OR, USA, 2–4 October 1995; pp. 98–101.

17. Lin, C.H.; Oshita, F.K.; Jennison, M.J.; Chang, P.C.; Wei, J.; Wilhelmi, C.; Bramlett, M.; Parkhurst, R.; Strathman, S.D.; Maple, M. Performances of CYTOPT™ low-k dielectric layer bridged GaAs-based enhancement mode pHEMT for wireless power application. *Solid-State Electron.* **2005**, *49*, 1708–1712.
18. Eldada, L. Polymer microphotronics. In *Nano- and Micro-Optics for Information Systems*; Eldada, L., Ed.; SPIE: Bellingham, WA, USA, 2003; Volume 5225, pp. 49–60.
19. Agnarsson, B.; Halldorsson, J.; Arnfinnsdottir, N.; Ingthorsson, S.; Gudjonsson, T.; Leosson, K. Fabrication of planar polymer waveguides for evanescent-wave sensing in aqueous environments. *Microelectron. Eng.* **2010**, *87*, 56–61.
20. Degenaar, P. A method for micrometer resolution patterning of primary culture neurons for SPM analysis. *J. Biochem.* **2001**, *130*, 367–376.
21. Agnarsson, B.; Jonsdottir, A.B.; Arnfinnsdottir, N.B.; Leosson, K. On-chip modulation of evanescent illumination and live-cell imaging with polymer waveguides. *Opt. Express* **2011**, *19*, 22929–22935.
22. Agnarsson, B.; Ingthorsson, S.; Gudjonsson, T.; Leosson, K. Evanescent-wave fluorescence microscopy using symmetric planar waveguides. *Opt. Express* **2009**, *17*, 5075–5082.
23. Vlachopoulou, M.; Tserepi, A.; Pavli, P.; Argitis, P.; Sanopoulou, M.; Misiakos, K. A low temperature surface modification assisted method for bonding plastic substrates. *J. Micromech. Microeng.* **2009**, *19*, 015007.
24. Halldorsson, J.; Arnfinnsdottir, N.B.; Jonsdottir, A.B.; Agnarsson, B.; Leosson, K. High index contrast polymer waveguide platform for integrated biophotonics. *Opt. Express* **2010**, *18*, 16217–16226.
25. Horvath, R.; Pedersen, H.C.; Larsen, N.B. Demonstration of reverse symmetry waveguide sensing in aqueous solutions. *Appl. Phys. Lett.* **2002**, *81*, 2166–2168.
26. Horvath, R.; Pedersen, H.C.; Skivesen, N.; Selmeczi, D.; Larsen, N.B. Optical waveguide sensor for on-line monitoring of bacteria. *Opt. Lett.* **2003**, *28*, 1233–1235.
27. Horvath, R.; Cottier, K.; Pedersen, H.C.; Ramsden, J.J. Multidepth screening of living cells using optical waveguides. *Biosens. Bioelectron.* **2008**, *24*, 799–804.
28. Grandin, H.M.; Städler, B.; Textor, M.; Vörös, J. Waveguide excitation fluorescence microscopy: A new tool for sensing and imaging the biointerface. *Biosens. Bioelectron.* **2006**, *21*, 1476–1482.
29. Schmitt, K.; Oehse, K.; Sulz, G.; Hoffmann, C. Evanescent field sensors based on tantalum pentoxide waveguides—A review. *Sensors* **2008**, *8*, 711–738.
30. Tiefenthaler, K.; Lukosz, W. Sensitivity of grating couplers as integrated-optical chemical sensors. *J. Opt. Soc. Am. B* **1989**, *6*, 209–220.
31. Dongre, C.; van Weerd, J.; Besselink, G.A.J.; Vazquez, R.M.; Osellame, R.; Cerullo, G.; van Weeghel, R.; van den Vlekkert, H.H.; Hoekstra, H.J.W.M.; Pollnau, M. Modulation-frequency encoded multi-color fluorescent DNA analysis in an optofluidic chip. *Lab Chip* **2011**, *11*, 679–683.
32. Ma, H.; Jen, A.K.Y.; Dalton, L.R. Polymer-based optical waveguides: Materials, processing and devices. *Adv. Mater.* **2002**, *14*, 1339–1365.

33. Vannahme, C.; Klinkhammer, S.; Christiansen, M.B.; Kolew, A.; Kristensen, A.; Lemmer, U.; Mappes, T. All-polymer organic semiconductor laser chips: Parallel fabrication and encapsulation. *Opt. Express* **2010**, *18*, 24881–24887.

© 2012 by the authors; licensee MDPI, Basel, Switzerland. This article is an open access article distributed under the terms and conditions of the Creative Commons Attribution license (<http://creativecommons.org/licenses/by/3.0/>).